Localization of the Unruh Effect

Kevin Player*

June 12, 2025

> The Unruh effect tells us that what we call particles is really just a matter of perspective.
>
> Lee Smolin

Abstract

We present a framework that interpolates between the standard thermal interpretation of the Unruh effect and a fully localized, non-thermal excitation. In a uniformly accelerating frame, the extended support of Rindler modes across the wedge leads to red- and blue-shifts, mixing frequencies in a way that gives rise to the familiar thermal response. To refine this picture, we introduce a partially localized perspective: by employing modular automorphisms, we map modes between nested Rindler wedges and analyze their localization properties. We further interpolate to compactly supported wave packets using parabolic cylinder functions, enabling a smooth transition from global to local behavior. Rather than attributing particle detection to the horizons thermality, this construction reframes the effect as the result of thrust, a localized, directed energy input into the field. This provides a mechanistic rather than statistical explanation for the observed radiation.

1 Introduction

The Unruh effect reveals that uniformly accelerated observers perceive the Minkowski vacuum as a thermal state, detecting a bath of particles where inertial observers see none. This phenomenon is usually derived by comparing positive-frequency Minkowski modes to Rindler modes, leading to Bogoliubov transformations that mix creation and annihilation operators. The standard explanation relies on the global nature of Rindler modes, which span the entire wedge and undergo both red-shift and blue-shift across their support.

In this work, we develop a complementary viewpoint by examining how localization affects the thermal character of the response. In Section 2, we begin with a review of the Unruh effect, including the relevant mode expansions and Bogoliubov transformations. In Section 3, we apply a standard source construction to inject particles into the field. When aimed at negative-frequency Unruh modes, this reproduces the Rindler particle spectrum predicted by the Bogoliubov transformation.

Section 4 explores partial localization by considering Rindler sub-wedges related by a space-like translations and reflections, corresponding to a modular automorphism of the associated von Neumann algebras. We then use parabolic cylinder functions to interpolate between eternal Rindler modes and fully localized wave packets. Finally, in Section 5, we interpret and discuss the implications of these results. This leads to a novel interpretation: the Unruh effect manifests as localized, non-thermal field excitations that act like a thrust-like driving force.

---

*kjplaye@gmail.com

2 Preliminaries

We draw notation and standard results from Frodden and Valdés [1].

Let $\hbar = c = 1$. We consider a uniformly accelerating observer in 1+1 dimensional Minkowski spacetime with metric signature $\eta = (-1, +1)$. The extension to 1+3 dimensions does not affect the key physics of the Unruh effect, so we restrict to the (t,x) plane where the boost is occurring.

Consider the free scalar massless Lagrangian

$$\mathcal{L}_{free} = -\frac{1}{2}\eta^{\mu\nu}\partial_\mu\phi\partial_\nu\phi. \tag{1}$$

We consider positive frequency modes with dispersion relation $\omega_k = |k| > 0$ as solutions to the resulting Klein-Gordon equation

$$\Box\phi = -\frac{\partial^2\phi}{\partial t^2} + \frac{\partial^2\phi}{\partial x^2} = 0, \tag{2}$$

where $\Box = \eta^{\mu\nu}\partial_\mu\partial_\nu$. We expand ϕ in terms of ladder operators $a_k, a_k^\dagger$

$$\phi(x,t) = \int \mathrm{d}k\, a_k \varphi_k(x,t) + \text{h.c.} \tag{3}$$

where

$$\varphi(x,t) = \frac{1}{\sqrt{4\pi\omega_k}}e^{i(kx-\omega_k t)}. \tag{4}$$

are pure Minkowkski positive frequency waves normalized with respect to the Klein-Gordon inner product over a Cauchy surface Σ (usually $t = 0$)

$$\langle f, g\rangle_{KG} = i\int_\Sigma \mathrm{d}x(f^*\partial_t g - \partial_t f^* g). \tag{5}$$

2.1 Rindler Coordinates

To describe the physics from the point of view of a uniformly accelerating observer, we introduce Rindler coordinates covering a right wedge

$$W = \{(x,t) : x > |t|\} \tag{6}$$

with apex at the origin, corresponding to region I pictured[1] in Figure 1; with coordinates

$$t = \frac{1}{a}e^{a\xi}\sinh(a\eta) \tag{7}$$

$$x = \frac{1}{a}e^{a\xi}\cosh(a\eta) \tag{8}$$

The constant acceleration parameter a is introduced explicitly to make the dependence of the Unruh temperature, $T = \frac{a}{2\pi}$, manifest in subsequent expressions. The coordinates (η, ξ) describe the proper time and position in the frame of a uniformly accelerating observer, with world-lines of constant ξ corresponding to hyperbolic trajectories in Minkowski spacetime.

The massless Klein-Gordon equation in Rindler coordinates is

$$\Box\phi = e^{-2a\xi}(-\partial_\eta^2 + \partial_\xi^2)\phi = 0 \tag{9}$$

---

[1] All diagrams follow the convention of t increasing upward and x increasing to the right.
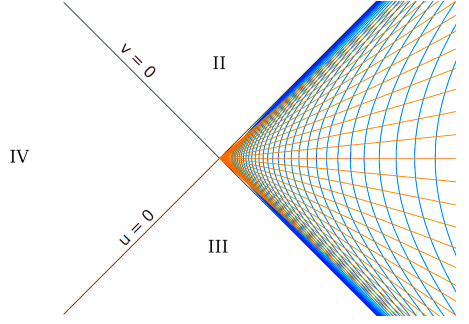
Figure 1: Rindler wedge I on the right.

The wave equation retains the same structure as the Minkowski case, up to the overall conformal factor $e^{-2a\xi}$. Since this factor does not affect the null structure of the equation, the mode solutions retain the same plane wave form but in the Rindler coordinates

$$r_k(\eta, \xi) = \frac{1}{\sqrt{4\pi\omega_k}}e^{-i(\omega_k\eta - k\xi)} + \text{h.c.} \tag{10}$$

for each wave number k and positive frequency $\omega_k = |k| > 0$. These "Rindler modes" are in terms of η and ξ and are thus confined to the Rindler wedge W. Since Rindler coordinates only cover region I (the right wedge), these modes are not defined globally in Minkowski space.

2.2 Unruh Modes

To understand how a uniformly accelerated observer perceives the Minkowski vacuum as a thermal bath, we construct the Unruh modes, analytic combinations of Rindler modes that correspond to positive-frequency solutions with respect to Minkowski time.

From now on let $\omega_k = k > 0$. Bogoliubov coefficients satisfy $\alpha_k^2 - \beta_k^2 = 1$, ensuring normalization. The expressions below reflect their standard form and the associated thermal weighting:

$$\alpha_k = \frac{e^{\frac{\pi\omega_k}{2a}}}{\sqrt{2\sinh\frac{\pi\omega_k}{a}}} = \sqrt{\frac{1}{1 - e^{-2\pi\omega_k/a}}}$$
$$\beta_k = \frac{e^{\frac{-\pi\omega_k}{2a}}}{\sqrt{2\sinh\frac{\pi\omega_k}{a}}} = \sqrt{\frac{1}{e^{2\pi\omega_k/a} - 1}} \quad \text{(thermal form)} \tag{11}$$

We analytically continue[2] the Rindler modes r_k and r_{-k} into the (t, x) plane, with $i\epsilon$ prescription, to understand their frequency content with respect to Minkowski time. This continuation reveals a change in frequency character (positive to negative) across the branch cut[3]

$$r_{+k} = \frac{1}{\sqrt{4\pi\omega_k}}e^{-i(\omega_k\eta - k\xi)} = \frac{1}{\sqrt{4\pi\omega_k}}(a(-t + x + i\epsilon))^{\frac{i\omega_k}{a}}$$
$$r_{-k} = \frac{1}{\sqrt{4\pi\omega_k}}e^{-i(\omega_k\eta + k\xi)} = \frac{1}{\sqrt{4\pi\omega_k}}(a(t + x - i\epsilon))^{\frac{-i\omega_k}{a}} \tag{12}$$

Although r_k and r_{-k} are positive-frequency modes with respect to Rindler time η, analytic continuation across the branch cut into the left wedge reveals that they acquire negative-frequency components with respect to Minkowski time t; see the middle column in Figure 2.

---

[2]From the definitions and properties of sinh and cosh, it follows that $a(\mp t + x) = e^{a(\pm\eta + \xi)}$.

[3]Specifically $r_{\pm k} = e^{\pm\frac{i\omega_k}{a}\log a(\mp t + x \pm i\epsilon)}$.

3

We recall the standard Minkowski positive-frequency plane wave modes, here with $k > 0$:

$$\varphi_{+k} = \frac{1}{\sqrt{4\pi\omega_k}} e^{-i(\omega_k t - kx)}$$

$$\varphi_{-k} = \frac{1}{\sqrt{4\pi\omega_k}} e^{-i(\omega_k t + kx)}$$

(13)

We next construct the Unruh modes

$$
\begin{aligned}
\mu_k^R &= \alpha_k r_{+k} + \beta_k \widetilde{r_{-k}^*} = \alpha_k r_{+k} - \beta_k l_{-k} \\
&= \frac{1}{\sqrt{4\pi\omega_k}\sqrt{2\sinh\frac{\pi\omega_k}{a}}} \left(e^{\frac{\pi\omega_k}{2a}} \left(a(-t+x+i\epsilon)\right)^{\frac{i\omega_k}{a}} + e^{\frac{-\pi\omega_k}{2a}} \left(a(t+x-i\epsilon)\right)^{\frac{i\omega_k}{a}} \right) \\
\mu_k^L &= \beta_k \widetilde{r_{+k}^*} + \alpha_k r_{-k} = -\beta_k l_{+k} + \alpha_k r_{-k} \\
&= \frac{1}{\sqrt{4\pi\omega_k}\sqrt{2\sinh\frac{\pi\omega_k}{a}}} \left(e^{\frac{-\pi\omega_k}{2a}} \left(a(-t+x+i\epsilon)\right)^{\frac{-i\omega_k}{a}} + e^{\frac{\pi\omega_k}{2a}} \left(a(t+x-i\epsilon)\right)^{\frac{-i\omega_k}{a}} \right)
\end{aligned}
$$

(14)

Here, the tilde denotes opposite analytic continuation across the logarithmic branch cut, corresponding to the conjugate $i\epsilon$ prescription. Operationally, this captures the mode's behavior in the left wedge and is often written using left Rindler modes l_k and l_{-k}, which have opposite sign and live in coordinates related by $t \to -t$, $x \to -x$.

The functions μ_k^R and μ_k^L are analytic in the lower-half complex t-plane and decay at infinity, so they qualify as positive-frequency Minkowski modes. They form an alternative orthonormal basis of solutions to the Klein-Gordon equation, distinct from the plane waves $\varphi_{\pm k}$. The Unruh modes diagonalize the Minkowski vacuum in terms of Rindler particle states and thus provide the natural framework for describing the Unruh effect and the thermal response perceived by uniformly accelerated observers.

2.3 Bogoliubov Transforms

We generalize the wedge W to a translated wedge W_c with apex $(0, c)$

$$W_c = \{(t, x) : x - c > |t|\}$$

(15)

and a reflected (left) wedge $\widetilde{W}_c$ with apex $(0, c)$

$$\widetilde{W}_c = \{(t, x) : x - c < -|t|\}.$$

(16)

Let the superscripts (0), (c), $(\widetilde{c})$, and (M) represent the W_0, W_c, $\widetilde{W}_c$, and Minkowski frames of reference respectively. Let $(A \to B)$ represent an open set inclusion $A \subseteq B$.

In the Haag-Kastler framework of algebraic quantum field theory, the assignment of von Neumann algebras to spacetime regions defines a covariant functor: the inclusion of regions $A \to B$ induces an inclusion of algebras $\mathcal{A}(A) \to \mathcal{A}(B)$. Conversely, the Bogoliubov transformation given by $\alpha^{(A \to B)}$ and $\beta^{(A \to B)}$ defines a contravariant functor, acting on algebras via pullback.

Since the analytically extended Rindler modes remain solutions of the Klein–Gordon equation, their inner products are preserved under continuation from the wedge to Minkowski space. This allows us to directly compute $W_0 \to M$ Bogoliubov coefficients from equation (14)

$$
\begin{bmatrix} a_k^{(0)} \\ a_{-k}^{(0)} \\ \hline a_k^{(0)\dagger} \\ a_{-k}^{(0)\dagger} \end{bmatrix} = \begin{bmatrix} \alpha_k & 0 & 0 & \beta_k \\ 0 & \alpha_k & \beta_k & 0 \\ \hline 0 & \beta_k & \alpha_k & 0 \\ \beta_k & 0 & 0 & \alpha_k \end{bmatrix}_{k,q} \begin{bmatrix} c_q^R \\ c_q^L \\ \hline c_q^{R\dagger} \\ c_q^{L\dagger} \end{bmatrix}
$$

(17)

for a change of basis from $a_q^{(M)}$ to c_q^R and c_q^L

$$\phi = \int dq \; \mu_q^R c_q^R + \mu_q^L c_q^L + \text{h.c.}$$

(18)

Figure 2: Spacetime diagrams of the $k > 0$ mode functions
$\begin{bmatrix} \varphi_k & r_k & \mu_k^R \\ \varphi_{-k} & r_{-k} & \mu_k^L \end{bmatrix}$. Color encodes the phase; brightness indicates magnitude. The Minkowski modes φ_k and Unruh modes μ_k display consistent *rainbow* phase structure at $t = 0$, reflecting their global positive-frequency character. In contrast, the Rindler modes r_k flip phase across the horizon due to the analytic structure of the logarithm. The left-moving mode r_k corresponds to emission; the right-moving r_{-k} to absorption.

So that we can summarize the transform as

$$a_k^{(0)} = \alpha_k c_q^R + \beta_k c_q^{L\dagger} \tag{19}$$

We next compute the more general mixed Bogoliubov transformations.

$$
\begin{aligned}
(c \to M): \quad a_k^{(c)} &= \int \mathrm{d}q \; \alpha_{kq}^{(c \to M)} a_q^M + \beta_{kq}^{(c \to M)} a_q^{(M)\dagger} \\
(c \to 0): \quad a_k^{(c)} &= \int \mathrm{d}q \; \alpha_{kq}^{(c \to 0)} a_q^{(0)} + \beta_{kq}^{(c \to 0)} a_q^{(0)\dagger} \\
(\widetilde{c} \to 0): \quad a_k^{(\widetilde{c})} &= \int \mathrm{d}q \; \alpha_{kq}^{(\widetilde{c} \to 0)} a_q^{(0)} + \beta_{kq}^{(\widetilde{c} \to 0)} a_q^{(0)\dagger}
\end{aligned}
\tag{20}
$$

We make use of a gamma function for $(c \to M)$. This occurs naturally in the KG dot product as an integral over an exponential phase from φ_k, and a $(x - c)$ power from $r_k^{(c)}$:

$$
\begin{aligned}
\alpha_{kq}^{(c \to M)} &= \left\langle \varphi_q, r_k^{(c)} \right\rangle = \frac{1}{a\pi} \sqrt{\frac{\omega_k}{\omega_q}} \left(\frac{a}{q} \right)^{\frac{i\omega_k}{a}} e^{\frac{\pi\omega_k}{a}} \Gamma\left(\frac{i\omega_k}{a} \right) \\
\beta_{kq}^{(c \to M)} &= \left\langle \varphi_q^*, r_k^{(c)} \right\rangle = \frac{1}{a\pi} \sqrt{\frac{\omega_k}{\omega_q}} \left(\frac{a}{q} \right)^{\frac{-i\omega_k}{a}} e^{\frac{-\pi\omega_k}{a}} \Gamma\left(\frac{-i\omega_k}{a} \right)
\end{aligned}
\tag{21}
$$

Next we consider products of shifted powers to go after $(c \to 0)$. We make use of a beta function for $(c \to 0)$ which occurs naturally in the KG dot product as an integral over a power of x and of $x - c$, from $r_k^{(0)}$ and $r_k^{(c)}$ respectively. We compute the Bogoliubov coefficients as

$$
\begin{aligned}
\alpha_{kq}^{(c \to 0)} &= \left\langle r_q^{(0)}, r_k^{(c)} \right\rangle = \frac{1}{2\pi a} \sqrt{\frac{\omega_k}{\omega_q}} (ac)^{\frac{i(\omega_k - \omega_q)}{a}} B\left(\frac{i\omega_k}{a}, \frac{-i(\omega_k - \omega_q)}{a} \right) \\
\beta_{kq}^{(c \to 0)} &= \left\langle r_q^{(0)*}, r_k^{(c)} \right\rangle = \frac{1}{2\pi a} \sqrt{\frac{\omega_k}{\omega_q}} (ac)^{\frac{i(\omega_k + \omega_q)}{a}} B\left(\frac{i\omega_k}{a}, \frac{-i(\omega_k + \omega_q)}{a} \right)
\end{aligned}
\tag{22}
$$

The reflected diamond wedge version also yields a beta function, but with a different form

$$
\alpha_{kq}^{(\widetilde{c}\to 0)} = \left\langle r_q^{(0)*}, r_k^{(\widetilde{c})} \right\rangle = \frac{1}{2\pi a} \frac{\sqrt{\omega_k \omega_q}}{\omega_q - \omega_k} (ac)^{\frac{i(\omega_k - \omega_q)}{a}} B\left(\frac{i\omega_k}{a}, -\frac{i\omega_q}{a}\right)
$$

$$
\beta_{kq}^{(\widetilde{c}\to 0)} = \left\langle r_q^{(0)}, r_k^{(\widetilde{c})} \right\rangle = \frac{1}{2\pi a} \frac{\sqrt{\omega_k \omega_q}}{\omega_q + \omega_k} (ac)^{\frac{i(\omega_k + \omega_q)}{a}} B\left(\frac{i\omega_k}{a}, \frac{i\omega_q}{a}\right)
$$

$$(23)$$

We can compare absolute magnitudes for M v.s. W_c and see that they don't depend on q or c

$$
\left|\beta_{kq}^{(c_1 \to M)}\right|^2 = \left|\beta_{kq}^{(c_2 \to M)}\right|^2
$$

$$
\left|\beta_{kq}^{(c_1 \to M)}\right|^2 = \left|\beta_{kq}^{(c_2 \to M)}\right|^2
$$

$$(24)$$

The c independence is expected since Unruh radiation is translation invariant. The q independence can be strengthened as the expected number of particles in mode k

$$
\int \mathrm{d}q \ \left|\beta_{kq}^{(c \to M)}\right|^2 = \frac{e^{\frac{-2\pi\omega_k}{a}}}{2\sinh\frac{\pi\omega_k}{a}} \int \mathrm{d}q \ \frac{2}{a\pi|q|}
$$

$$(25)$$

where we factor out the divergent part to recover the radiation equation again[4].

We next turn to $(c \to 0)$ and also find c independence there

$$
\left|\alpha_{kq}^{(c_1 \to 0)}\right| = \left|\alpha_{kq}^{(c_2 \to 0)}\right|
$$

$$
\left|\beta_{kq}^{(c_1 \to 0)}\right| = \left|\beta_{kq}^{(c_2 \to 0)}\right|
$$

$$(26)$$

which is somewhat more surprising since this implies that $\int \mathrm{d}q \ \left|\beta_{kq}^{(c_2 \to c_1)}\right|^2$ are c_1 and c_2 independent quantities for every shifted (and reflected resp.) wedge inclusion.

In other words, for shifted wedges[5], the expected number of particles for a mode $r_k^{(c_2)}$ of W_{c_2} in W_{c_1}'s vacuum is independent of the choice of shift c_2 and c_1. More explicitly we have a transform matrix of Λ_c from W_0 to W_c

$$
\begin{bmatrix} a_k^{(c)} \\ a_{-k}^{(c)} \\ a_k^{(c)\dagger} \\ a_{-k}^{(c)\dagger} \end{bmatrix} = \underbrace{\left[\begin{array}{cc|cc} A_c & 0 & B_c & 0 \\ 0 & -A_c & 0 & -B_c \\ \hline \overline{B_c} & 0 & \overline{A_c} & 0 \\ 0 & -\overline{B_c} & 0 & -\overline{A_c} \end{array} \right]_{k,q}}_{\Lambda_c} \begin{bmatrix} a_q^{(0)} \\ a_{-q}^{(0)} \\ a_q^{(0)\dagger} \\ a_{-q}^{(0)\dagger} \end{bmatrix}
$$

$$(27)$$

where $A_c = \alpha_{kq}^{(c \to 0)} = P_c A_1 P_c^{-1}$ and $B_c = \beta_{kq}^{(c \to 0)} = P_c B_1 P_c$ for a diagonal phase factor matrix

$$
P_c = P_{c,rs} = \delta(r-s) c^{\frac{i\omega_r}{a}} = e^{\frac{iH}{a}\log c}
$$

$$(28)$$

We can write Λ_c out compactly out as

$$
\Lambda_c = Q_c \Lambda_1 Q_c^{-1}
$$

$$(29)$$

where

$$
Q_c = \begin{bmatrix} P_c, & 0 & 0 & 0 \\ 0 & P_c & 0 & 0 \\ 0 & 0 & P_c^{-1} & 0 \\ 0 & 0 & 0 & P_c^{-1} \end{bmatrix}
$$

$$(30)$$

---

[4]We frequently use here and elsewhere $|\Gamma(ib)|^2 = \frac{\pi}{b\sinh\pi b}$

[5]Similar statements are true for reflected (diamond) wedge inclusions

Note that $\lim_{c \to 0} \Lambda_c = 1$ since the limit of $\lim_{c \to 0} \alpha_{kq}^{(c \to 0)} = 1$ and $\lim_{c \to 0} \beta_{kq}^{(c \to 0)} = 0$, which corresponds nicely to $\lim_{c \to 0} W_c = W_0$. The composition of Bogoliubov transforms, $\Lambda_{nc} = \Lambda_c^n$, yields

$$
\begin{aligned}
Q_{nc} \Lambda_1 Q_{nc}^{-1} &= \Lambda_{nc} \\
&= (Q_c \Lambda_c Q_c) \left(Q_c^{-1} \Lambda_c Q_c \right) \cdots (Q_c \Lambda_c Q_c) \\
&= Q_c \Lambda_c^n Q_c^{-1}
\end{aligned}
\tag{31}
$$

so that

$$
\begin{aligned}
\Lambda_c^n &= Q_c^{-1} Q_{nc} \Lambda_1 Q_{nc}^{-1} Q_c \\
&= Q_n \Lambda_1 Q_n^{-1}
\end{aligned}
\tag{32}
$$

and more generally we have a one parameter group given by

$$
\left\{ \Lambda_0^x = Q_x \Lambda_0 Q_x^{-1} : x \in \mathbb{R} \right\}.
\tag{33}
$$

These Bogoliubov transformations between shifted wedges define a one-parameter group, reflecting an underlying symmetry structure. This naturally connects to modular flow as studied in algebraic QFT, where such transformations correspond to automorphisms generated by the modular operator. This is an explicit realization of modular flow, due to the von Neumann algebra modular automorphism associated with the translation $W_0 \to W_c$, studied in detail in Tomita-Takesaki theory [2]. There we find thermal KMS states between open set inclusions in a much more general setting.

Consider a sequence

$$
W_{c_n} \subseteq \cdots \subseteq W_{c_i} \subseteq \cdots \subseteq W_{c_j} \subseteq W_{c_2} \subseteq W_{c_1}
\tag{34}
$$

Then each $W_{c_i} \subseteq W_{c_j}$ involves particle production with a fixed squared magnitude for mode k. We calculate this expected number of W_{c_i} particles for mode k in W_{c_j}'s vacuum

$$
\langle 0_{W_{c_j}} | a_k^{(c_i)\dagger} a_k^{(c_i)} | 0_{W_{c_j}} \rangle = \frac{1}{2\pi^2 k \sinh \frac{\pi k}{a}} \int_{x=0}^{\infty} \frac{x \sinh x}{(x + \frac{\pi k}{a}) \sinh(x + \frac{\pi k}{a})}
\tag{35}
$$

which diverges. The integrand goes to $e^{-\frac{\pi k}{a}}$ as x gets large, so we can see that the expected number of particles in ratio goes to another thermal form

$$
\frac{1}{m(e^{2m} + 1)} = \frac{1}{k(e^{\frac{2\pi \omega_k}{a}} - 1)}.
\tag{36}
$$

3 Driving Sources

We now ask a fundamental question: **"What exactly is accelerating the observer?"** Until this point, we've treated acceleration as a coordinate choice, without invoking any underlying physical mechanism. We have also not specified the observer's precise location within the Rindler wedge, nor the spatial origin of the observed excitations. These ambiguities reflect the effective coarse-graining over the observer's details, a feature that contributes to the thermal character of the Unruh effect.

Figure 3 illustrates the situation for a sharply peaked frequency wave packet made of Rindler modes. The modes r_k are left-moving, propagating toward the future horizon and are interpreted as **emission**. The r_{-k} modes are right-moving, originating from the past horizon and are interpreted as **absorption**. The Rindler modes are constructed as superpositions of Minkowski modes φ_q, effectively smeared over a range of frequencies. This is visually evident in Figure 2, where the local frequencies increase (blue-shift) near the horizons. This is made explicitly by the Bogoliubov coefficients $\alpha_{kq}^{(c \to M)}$ and $\beta_{kq}^{(c \to M)}$ which encode the Fourier decomposition of the Rindler modes through their Klein-Gordon

Figure 3: A Rindler mode's frequency is smeared out in Minkowski space, blue-shifted near the horizon. We diagram a particle as if it were striking a mirror at the rear of a rocket, where its reflection emerges as a combination of emission and absorption processes in the Rindler frame.

inner products with the Minkowski modes φ_q and φ_q^*, respectively. This frequency de-localization, tied to the observer's acceleration horizon, underlies the apparent thermal character of the radiation.

To address this, we introduce a driving source, a physical mechanism responsible for the field's excitation and, indirectly, for the observer's acceleration. This reframes the interpretation: the radiation is not spontaneous but instead emerges as a coherent response to the source, see illustration in Figure 4. The apparent thermality, then, is tied to our ignorance of the source's detailed structure.

We aim to encode the effect of a creation operator by introducing a source term $J(x)$ into the Lagrangian at some distant time in the past, which directly excites the field in a specific mode. Since $J(x)$ couples linearly, it prepares a coherent state that excites the chosen mode in a controlled, phase-coherent manner. To replicate the action of a creation operator, the source must be engineered such that its overlap with the mode functions $u_k(x)$ matches the operator's action on the field.
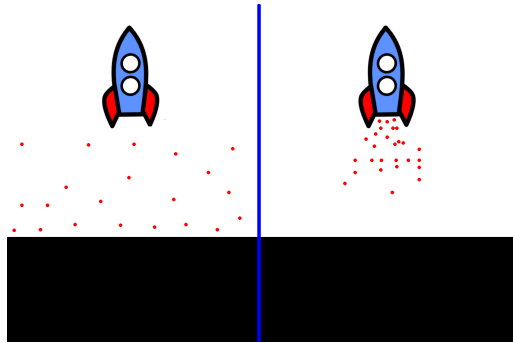

Figure 4: Conceptual illustration of thermal v.s. localized acceleration.

The field can be expanded as in equation (18), and the β_k-term in equation (19) is responsible for the thermal particle content of the Minkowski vacuum as seen by Rindler observers. For clarity, we first present the construction for a single positive-frequency μ_k^{L*}-mode. Because the Unruh modes form a complete orthonormal set under the Klein-Gordon inner product, this construction extends linearly and independently to the full

8

family of modes. We encode the effect of a creation operator $c_k^{L\dagger}$ using

$$c_k^{L\dagger} = \langle \phi, \mu_k^{L*} \rangle_{KG} = \int \mathrm{d}x\ \mu_k^{L*}(x)\phi(x) \tag{37}$$

and the orthogonality of the mode functions in the Klein-Gordon inner product.

Although the Unruh modes involve both left- and right-moving Rindler components, associated with emission and absorption in the accelerated frame, they are constructed to have purely negative frequency with respect to Minkowski time. This ensures that the source couples to physical creation operators and injects particles into the field in a well-defined way. The resulting excitation respects the correct Minkowski vacuum structure while encoding the full Rindler response.

In the generating functional formalism, setting $J_k^L(x) = -\beta_k u_k^{L*}$ the functional derivative $\frac{\delta}{\delta J_k^L} Z[J_k^L]|_{J_k^L=0}$ inserts ϕ into time-ordered correlators. Smearing this field insertion against $\mu_k^{L*}(x)$ thus projects onto $c_k^{L\dagger}$ and we have[6]

$$\begin{aligned} a_k^{(0)J} &= \alpha_k c_q^R + \beta_k c_q^{L\dagger} - \beta_k c_q^{L\dagger} \\ &= \alpha_k c_q^R \end{aligned} \tag{38}$$

In Rindler coordinates, this source term prepares a modified field state in which the Rindler mode occupation differs from the thermal distribution of the Minkowski vacuum. Rather than simply adding energy, the source introduces a coherent excitation that cancels the mode structure induced by the Bogoliubov β-terms, effectively replacing their contribution. This lets us construct a state where the Rindler response is vacuum-like for mode k

$$\langle J_k^L| b_k^\dagger b_k |J_k^L\rangle = \langle 0_M| b_k^{J_k^L\dagger} b_k^{J_k^L} |0_M\rangle = 0 \tag{39}$$

As a result, the source reproduces the exact Rindler particle spectrum predicted by the Rindler–Minkowski Bogoliubov transformation, provided the excited modes are drawn from a Klein-Gordon orthonormal basis such as the Unruh modes; this holds when using causal (retarded) or time-ordered (Feynman) Green's functions, both of which allow linear superpositions of negative-frequency modes to generate particle injection.

4   Subwedge Localization in Rindler Space

4.1   Localization via Translated Wedge Inclusion

Consider the two nested Rindler wedges $W_c \subseteq W_0$ shown in Figure 5. Let r_q denote a Rindler mode associated with W_0, analytically continued to the entire Minkowski space. The gray-scale region indicates the full support of r_q, while the rainbow-colored segment shows its restriction to the smaller wedge W_c.

By considering the restriction of r_q to W_c, we have partially localized the observer and the mode. The restriction effectively cuts off the high-frequency content of r_q near the future horizon[7]. The resulting mode still spans the full spatial extent of W_c, but it is now insulated from the highly oscillatory behavior near the horizons of W_0. The localization is not complete however, the observer can still be anywhere within the wedge W_c, and the corresponding modes r_k still exhibit thermal characteristics because of low-frequency oscillations extending throughout the wedge.

---

[6]The remaining α_k factor reflects the mismatch between the squeezed Unruh vacuum and the coherent state prepared by the source.

[7]Similarly, r_{-q} experiences suppression near the past horizon.
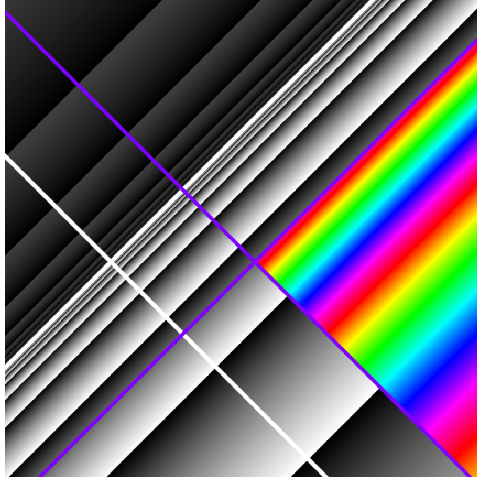
Figure 5: A Wedge W_c (blue) inside of the wedge W_0 (white). Rindler mode r_q of W_0 (gray-scale) restricted to W_c (rainbow).

To further study the situation, consider the modulus squared inner product $\left|\left\langle r_q^{(0)}, r_k^{(c)} \right\rangle\right|^2$, also known as the Bogoliubov $\left|\alpha_{kq}^{(c\to 0)}\right|^2$, from equation (22). We fix q and view

$$\left|\left\langle r_q^{(0)}, r_k^{(c)} \right\rangle\right|^2 = \frac{\sinh\frac{\pi\omega_q}{a}}{4\pi a(\omega_q - \omega_k)\sinh\frac{\omega_q - \omega_k}{a}\sinh\frac{\pi\omega_k}{a}} \tag{40}$$

as a function of ω_k. The function exhibits a second-order pole at $\omega_k = \omega_q$, resulting in a sharply peaked spectral response, see Figure 6. The thermal character is evident in the sinh terms: $\sinh\frac{\pi\omega_k}{a}$ introduces a broadening near $\omega_k = 0$, while $\sinh\frac{\omega_q - \omega_k}{a}$ contributes thermal spreading near the peak at $\omega_k = \omega_q$. However, the pronounced spectral peak at $\omega_k = \omega_q$ arises not from thermal effects but from the localization itself.
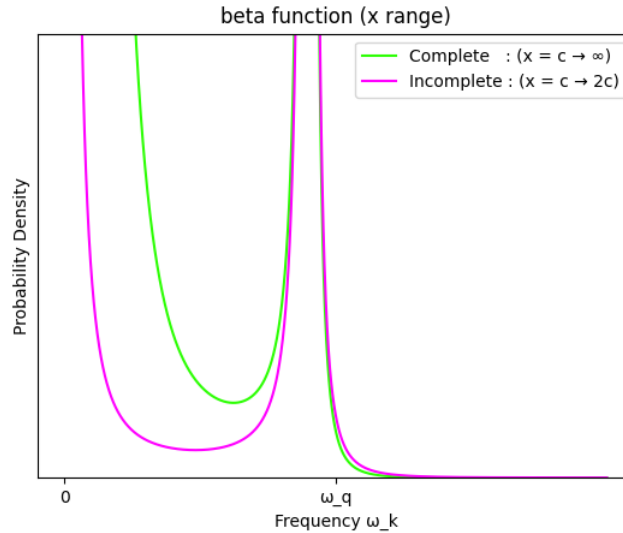

Figure 6: The Rindler modes r_k of W_c show a peaked spectral overlap with r_q at $\omega_k = \omega_q$. The incomplete beta function picks out the spectral peak supressing the peak at zero.

10

4.2 Diamond Localization via Reflected Wedge Intersection

Further localization is achieved by intersecting W_c with a reflected wedge $\widetilde{W}_{2c}$. This defines a more tightly localized diamond-shaped region, as shown in Figure 7. The mode r_q is now restricted to the intersection $W_c \cap \widetilde{W}_{2c}$, which eliminates much of the infrared divergence previously associated with the unrestricted wedge.

The Klein Gordon inner product at $t = 0$ now takes the form of an incomplete version of the beta function from equation (22), corresponding to an integral[8] evaluated from c to $2c$ rather than extending to infinity. This inner product does not however coorospond to a mode expansion of the field, since the analytic continuation of the diamond would be to all of W_c, or all of $\widetilde{W}_{2c}$, in which case we would no longer be localized to the diamond. So it is no longer invariant to integrate along a Cauchy surface for the inner product; this construction does not define a complete orthonormal set, and cannot be used to build a full basis of field modes.

Instead, we can take the viewpoint that the diamond is a localized driving source, as in Section 3; we are no longer interpreting r_q as a solution to the free Klein-Gordon equation everywhere, but as a compact test function that drives a response in the field. We turn on r_q exactly for a fixed period of $x - t$ (or $x + t$ for r_{-q}). The resulting spectral response in the diamond, computed from this truncated integral, is shown in Figure 6. The plot reveals that the main spectral peak at $\omega_k = \omega_q$ persists, while the thermal contribution near $\omega = 0$ is significantly attenuated.
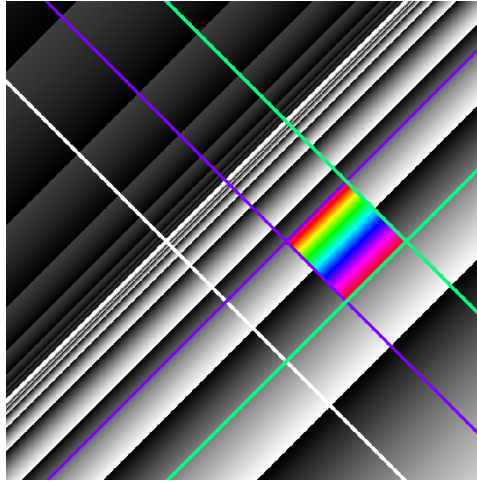

Figure 7: The same situation as in Figure 5 but we further intersect with a reflected (left) wedge $\widetilde{W}_{2c}$ (green). Rindler mode r_q of W_0 (gray-scale) restricted to $W_c \cap \widetilde{W}_{2c}$ (rainbow).

4.3 Wave Packet Interpolation

Let $N = e^{-\frac{1}{2}\frac{(x-t-\mu)^2}{\sigma^2}}$ be a Gaussian kernel that we will use to shape a wave packet[9]. Then using the Parabolic cylindrical function[10] $D_\nu(z)$ we have

$$\langle \varphi_q N, r_k \rangle = \frac{1}{2\pi a}\sqrt{\frac{\omega_k}{\omega_q}}(\sigma a)^{\frac{i\omega_k}{a}}e^{-\frac{1}{4}z^2}e^{-\frac{1}{2}iq}\Gamma(-\nu)D_\nu(z) \qquad (41)$$

---

[8]We could also use the beta function in equation (23) to compute the same inner product using the alternative incomplete beta function.

[9]We multiply φ by N but we could just as easily multiply r_k by N for the same effect.

[10]$\int_{t=0}^{\infty} e^{-zt}t^{a-\frac{1}{2}}e^{-\frac{1}{2}t^2}\mathrm{d}t = e^{\frac{1}{4}z^2}\Gamma\left(a + \frac{1}{2}\right)D_{-a-\frac{1}{2}}(z)$, and $U(a, z) = D_{-a-\frac{1}{2}}(z)$
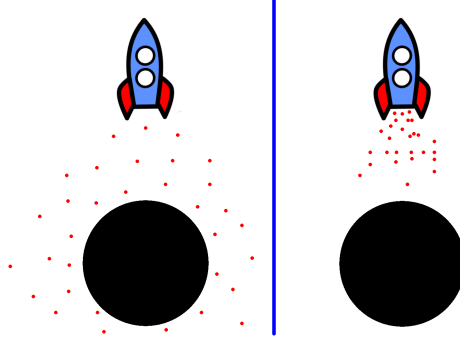
Figure 8: Conceptual illustration of thermal Hawking radiation v.s. local acceleration.

for $\nu = -\frac{i\omega_k}{a}$ and $-z = iq\sigma - \frac{\mu}{\sigma}$. And then

$$|\langle\varphi_q N, r_k\rangle|^2 = \frac{\omega_k}{4\pi^2 a^2 \omega_q}\left|e^{-\frac{1}{2}z^2}\right| |\Gamma(-\nu)|^2 |D_\nu(z)|^2 \tag{42}$$

From [3] we have

$$D_\nu(-z) = e^{-i\pi\nu}z^\nu e^{-\frac{1}{4}z^2}\{1+O(|z|^{-2})\} + \frac{(2\pi)^{\frac{1}{2}}}{\Gamma(-\nu)}z^{-\nu-1}e^{\frac{1}{4}z^2}\{1+O(|z|^{-2})\} \tag{43}$$

when $-\frac{3}{4}\pi+\epsilon \leq \arg z \leq \frac{1}{4}\pi-\epsilon$. The second $e^{\frac{1}{4}z^2}$ term dominates for $z \to \infty$ as $\sigma \to 0$ and the first $e^{-\frac{1}{4}z^2}$ term dominates for $z \to -i\infty$ as $\sigma \to \infty$. This is the Stokes phenomenon which flips over as we cross the Stokes line $\arg z = -\frac{\pi}{4}$. The situation is pictured in Figure 9. Combining equations (42) and (43) we find that the asymptotics of the inner product interpolate between a thermal character and a localized character.

$$|\langle\varphi_q N, r_k\rangle|^2 \to \begin{cases} \frac{1}{4\pi a\omega_q}\frac{z^{2\nu}\left|e^{-z^2}\right|}{\sinh\frac{\pi\omega_k}{a}} & \text{as} \quad \sigma \to \infty \\ \frac{\omega_k}{2\pi a^2\omega_q}z^{-\nu-1} & \text{as} \quad \sigma \to 0 \end{cases} \tag{44}$$
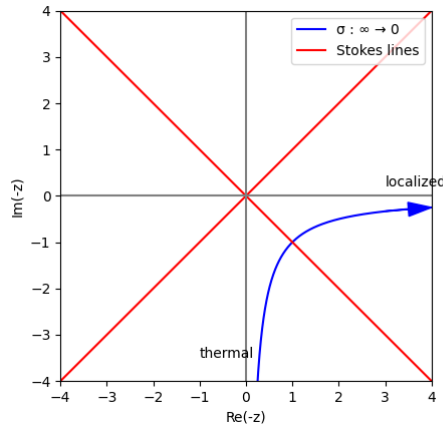

Figure 9: Stokes phenomenon for the Parabolic Cylinder Function as σ interpolates between ∞ and 0. The Stokes curves is passed at $\arg z = -\frac{\pi}{4}$.

5 Conclusion and Prediction

This work reframes the Unruh effect as a localized, detector-based response to directed energy input, such as acceleration-induced coupling—rather than as a consequence of global horizon thermality. By restricting Rindler modes to sub-wedge regions and their intersections, motivated by modular theory, we demonstrate that apparent thermal behavior can emerge from non-local mode mixing rather than a thermal density matrix. Using parabolic cylinder functions, we construct smooth, spatially localized wave packets that interpolate between global and compact support, revealing how detector response depends sensitively on localization scale. Although our results are developed in flat spacetime, the equivalence principle suggests a natural extension to curved spacetimes. In particular, this framework may shed light on Hawking radiation by modeling localized excitations near black hole horizons, as illustrated in Figure 8.

6 Acknowledgments

7 Notes

To go after $(c \to M)$ we start with a useful formula obtained by taming Fourier oscillations and doing contour integrals

$$\int_{-\infty}^{\infty} e^{ikx}(x \pm i\epsilon)^b \mathrm{d}x = -\frac{2i}{k^{b+1}} e^{\frac{-\pi b}{2}} \Gamma(b+1) \tag{45}$$

$$\int_{c}^{\infty} x^a (x-c)^b \mathrm{d}x = c^{a+b+1} B(b+1, -a-b-1) \tag{46}$$

and over sign choices $b, d \in \{-1, 1\}$

$$f_{k,b,d} = \left(a \left(b(t - i\epsilon) + x \right) \right)^{\frac{id\omega_k}{a}} \tag{47}$$

we have the dot product

$$\left\langle f_{k,b_k,d_k}, f_{q,d_q,d_q} \right\rangle = \frac{1}{2\pi} \sqrt{\frac{\omega_k}{\omega_q}} (ac)^{\frac{i(d_k\omega_k - d_q\omega_q)}{a}} \left((-d_k) \frac{b_k + b_q}{2} \right) B \left(\frac{id_k\omega_k}{a}, \frac{-i(d_k\omega_k - d_q\omega_q)}{a} \right) \tag{48}$$

References

[1] E. Frodden and N. Valdés, "Unruh effect: Introductory notes to quantum effects for accelerated observers," *International Journal of Modern Physics A*, vol. 33, p. 1830026, sep 2018.

[2] H.-J. Borchers, "On revolutionizing quantum field theory with tomita's modular theory," *Journal of Mathematical Physics*, vol. 41, no. 6, pp. 3604–3673, 2000.

[3] F. W. J. Olver, "Uniform asymptotic expansions for weber parabolic cylinder functions of large orders," *Journal of Research of the National Bureau of Standards. Section B, Mathematical Sciences*, vol. 63B, pp. 131–169, 1959.